American Mineralogist, Volume 72, pages 345–352, 1987

Mineralogy of triple- and double-chain pyriboles from Orijärvi, southwest Finland

JOHN C. SCHUMACHER, MICHAEL CZANK
Mineralogisches Institut, Olshausenstrasse 40, D-2300 Kiel, Federal Republic of Germany

ABSTRACT

Pyriboles that consist of mixed double chains (anthophyllite), alternating double and triple chains (chesterite), and triple chains (jimthompsonite) coexist with phlogopite and Zn-rich spinel at Orijärvi, southwestern Finland. Each of these three pyribole-structure types has been observed as lamellae as wide as a few thousand ångströms, and electron-diffraction photographs give strong and sharp reflections for all three of these phases. However, the pyriboles are predominantly composed of large disordered areas, in which the proportions of triple-chain units to double-chain units are highly variable. Electron-microprobe analyses indicate that SiO_2, Al_2O_3, and Na_2O increase and FeO and CaO decrease in the jimthompsonite relative to the anthophyllite. These chemical variations can be explained by different proportions of A sites, octahedral sites, and tetrahedral sites in the double- and triple-chain structures.

Assuming that Fe^{2+} and Mg are partitioned similarly between the distorted octahedral (dM) and regular octahedral (rM) sites of the anthophyllite and the jimthompsonite, the differing proportions of dM and rM in the two structures allow the estimation of site occupancies and the calculation of an intersite distribution coefficient $(K_d)^{dM\text{-}rM}_{Fe\text{-}Mg} = 13.868$. On the basis of the work of Seifert (1977), this value suggests a metamorphic temperature of about 600°C, which is consistent with the 550 to 630°C estimated for this area by Schreurs (1985).

INTRODUCTION

Naturally occurring pyriboles (see Veblen, 1981) were reported by Veblen and Burnham (1975, 1976) from a metamorphosed ultramafic body at Chester, Vermont, U.S.A. Orthorhombic pyriboles, with silicate triple chains are named jimthompsonite (the monoclinic polymorph is clinojimthompsonite), and ordered sequences of alternating double and triple chains are called chesterite (Veblen and Burnham, 1978a, 1978b).

In addition to the Chester occurrence, small domains of jimthompsonite have been reported in hydrothermally altered ultramafic rocks from Valle Maggia, Switzerland (Nissen et al., 1979), and clinojimthompsonite-like lamellae have been reported in altered augite by Nakajima and Ribbe (1980), Veblen and Buseck (1981), and Akai (1982). Intergrowths of Ca pyribole and actinolite have been reported by Yau and Peacor (1985). Chesterite-like lamellae have been reported in anthophyllite (Cressey et al., 1980), and triple-chain lamellae have been reported in grunerite asbestos (Whittaker et al., 1981a, 1981b).

The pyriboles found at Orijärvi are a new occurrence of triple-chain silicates. This locality, well known for cordierite-anthophyllite and the site of sulfide mineralization, represents a new paragenesis for triple-chain pyriboles, as the previous occurrences are either from metamorphosed ultramafic bodies or altered Ca pyroxenes.

Chemical analyses of jimthompsonite are rarer than its occurrence. In the Orijärvi samples, it was possible to obtain analyses that approximate the anthophyllite (double-chain) and jimthompsonite (triple-chain) parts of the disordered pyribole crystals. This paper describes the pyriboles from Orijärvi and discusses chemical variations between the anthophyllite and jimthompsonite parts of grains.

GEOLOGIC SETTING AND SAMPLE DESCRIPTION

Since the classic study by Eskola (1914), the Orijärvi area in southwest Finland has been known as a locality of cordierite-anthophyllite rocks and sulfide mineralization. The rocks around the Orijärvi mine are chiefly Precambrian felsic and mafic volcanic rocks with minor calcareous horizons that were metamorphosed during the Svecofennian orogeny about 1800 Ma (Simonen, 1980). Recent work by Schreurs (1985) suggests peak metamorphic conditions of about 550–630°C and pressures of 3–5 kbar. The sulfide mineralization probably occurred during a phase of premetamorphic hydrothermal alteration by sea water (Berge, 1978). In addition, this process provides a likely mechanism for producing the protoliths of cordierite-anthophyllite rocks from normal basalts (Berge, 1978; Robinson et al., 1982; Schumacher, 1983).

The pyribole-bearing sample was collected from the mine spoil piles near the unpaved road due west of the

0003–004X/87/0304–0345$02.00

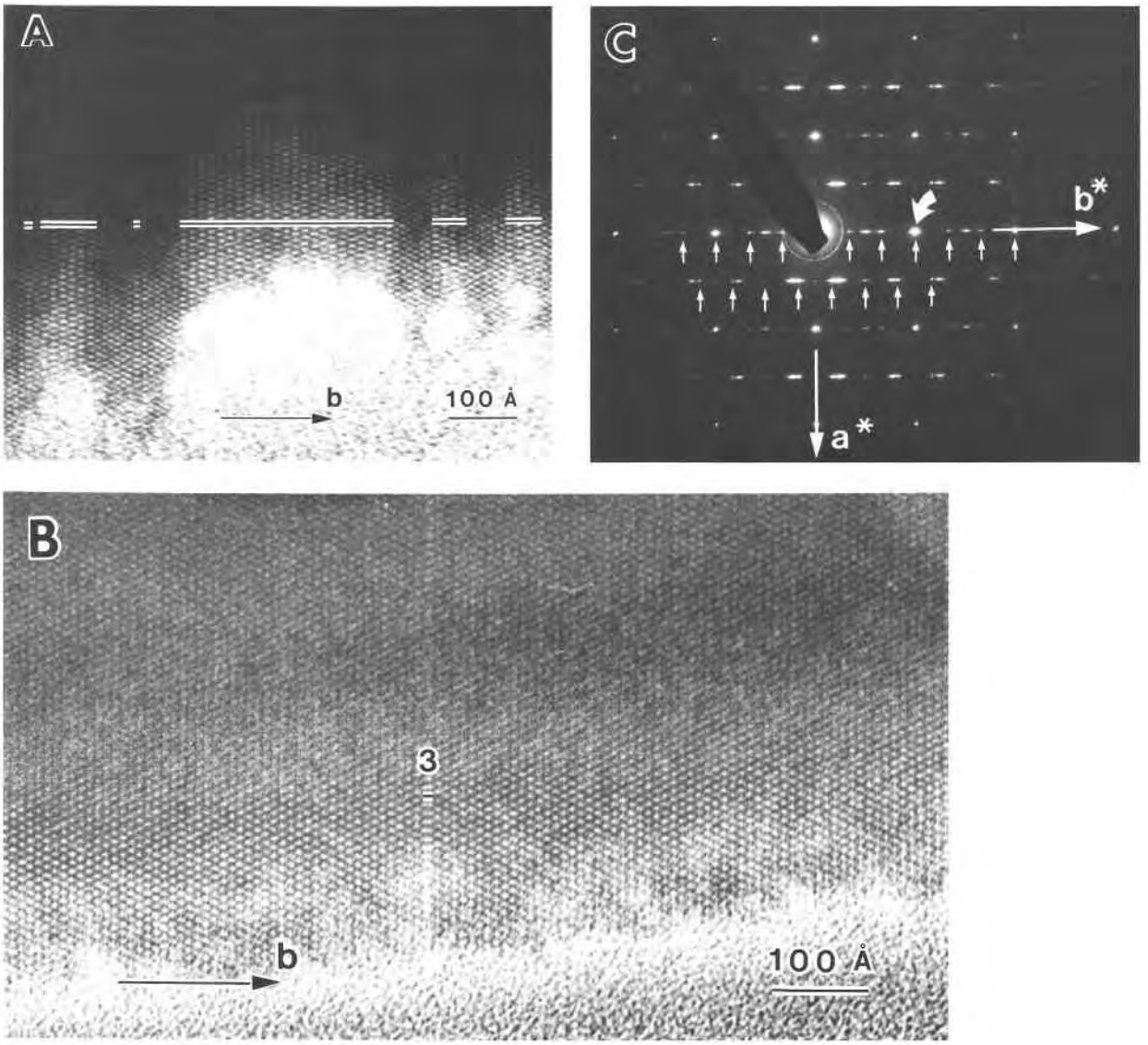

Fig. 1. Bright-field images of biopyriboles in [001] projections (A, B) and a selected-area electron-diffraction pattern of the pyribole (C), which includes the areas shown in parts A and B. Bars in parts A and B denote triple-chain regions, and unmarked areas are double-chain regions. (A) Region rich in triple-chain units. (B) Region rich in double-chain units. (C) Light arrows denote diffraction maxima of triple-chain units, and the heavy arrow marks a diffraction maximum common to anthophyllite (040) and jimthompsonite (060).

main pit at the Orijärvi mine. The hand specimen that contains the pyriboles seems to be composed chiefly of amphibole, lesser amounts of phlogopite, minor green spinel, and minor galena. The "amphiboles" are white to pale green and appear as randomly oriented sprays or bundles of prismatic crystals less than 4 mm long. The phlogopite is black to dark brown, and the flakes are generally less than about 5 mm across.

Thin sections of this sample show that it is composed chiefly of pyribole and subordinate phlogopite, with minor spinel and an opaque phase (galena). The phlogopite forms interstitially between subhedral pyribole grains. The anhedral pale-green spinels occur in roughly circular clusters that are generally less than 3.0 mm across; they seem to have grown in the interstices of the pyribole grains and may be connected in three dimensions.

Mineralogy of associated phases

Methods

Microprobe analyses were done on polished thin sections on the Cameca electron microprobe (Camebax Micro) at the Mineralogical Institute at Christian Albrechts University in Kiel, Federal Republic of Germany. Operating conditions were 20 kV and 20 nA. Data reduction was done using the atomic number, absorption, and fluorescence correction (ZAF) that is provided by Cameca.

TABLE 1. Representative analyses of phlogopite and spinel

Phlogopite				Spinel			
	wt%		Cations per 11 oxygens		wt%		Cations per 4 oxygens
SiO_2	43.53	Si	3.006	SiO_2	0.00	Al	2.002
TiO_2	0.50	Al	0.994	TiO_2	0.00		
Al_2O_3	14.13	Sum	4.000	Al_2O_3	60.10	Mg	0.281
Cr_2O_3	0.01			Cr_2O_3	0.00	Fe^{2+}	0.148
FeO	3.81	Al	0.156	FeO	6.26	Mn	0.000
MnO	0.00	Ti	0.026	MnO	0.02	Zn	0.568
MgO	24.93	Cr	0.001	MgO	6.68	Total	4.002
NiO	0.00	Mg	2.567	NiO	0.00		
ZnO	0.09	Fe^{2+}	0.220	ZnO	27.20		
CaO	0.00	Zn	0.005	CaO	0.00	X_{Mg}	0.655
Na_2O	0.81	□	0.025	Na_2O	0.00		
K_2O	8.27	Sum	2.975	K_2O	0.00		
Total	96.08	Na	0.108	Total	100.26		
		K	0.729				
		□	0.163				
		Sum	0.837				
		Total	7.812				
		X_{Mg}	0.921				

Note: Oxides in weight percent. Open boxes represent vacant sites and are not counted in the summation of the cation sites (sum) or in the cation total. X_{Mg} = Mg/(Mg + Fe).

The high-resolution transmission-electron microscopy (HRTEM) was done on the same grain from the same thin section that was used for the microprobe study. The sample was thinned by ion bombardment and placed in a rotating and tilting stage for use in the Phillips EM 400T electron microscope, which was operated at 100 kV. The photomicrographs shown in Figures 1 and 3 were taken under conditions described by Buseck and Iijima (1974). The image interpretation follows that of Veblen and Buseck (1979).

Phlogopite and spinel

In thin section the phlogopites are anhedral and are pleochroic from colorless to pale brown. Individual phlogopite flakes rarely exceed 2.5 mm in the thin sections. Microprobe analyses show the phlogopite to be homogeneous; representative analyses are given in Table 1. The Na/(Na + K) ratio of 0.13 is higher than that of most of the phlogopites coexisting with wonesite that have been described by Spear et al. (1981); however, the interlayer vacancy (=0.163) in the phlogopite from this study is lower than in the phlogopites described by Spear et al. (1981). The anhedral pale blue-green spinels are less than 0.4 mm across, and some partially enclose subhedral pyribole grains (Table 1).

WIDE-CHAIN PYRIBOLES

Properties in thin sections

The pyribole grains are subhedral and prismatic, the largest grains being 3.2 by 0.3 mm. They have straight extinction and are colorless in plane-polarized light. In general, these pyriboles appear identical to those of Veblen et al. (1977, see also cover illustration) and Veblen and Burnham (1978a). All the sections parallel to **c** show (001) parting that is perpendicular to the edges of the grains, as commonly observed in orthorhombic amphiboles. End sections [cut parallel (001)] that are viewed with crossed polars show conspicuous lamellae that are oriented parallel to (010) of the pyribole. Conoscopic images obtained by scanning across the lamellae in grains that are oriented to give optic-axis figures show that the optic axial angle ($2V$) changes rapidly from a large positive value, typical of anthophyllite, to a slightly smaller negative one, typical of triple-chain pyriboles (Veblen and Burnham, 1978a). In areas of the crystals with high concentrations of different lamellae, the isogyre "zigzags" across the field of view.

HRTEM images

The HRTEM images (Fig. 1) confirm the presence of interlayers of triple and double chains in the pyribole grains. Following the contrast interpretation of Veblen and Buseck (1979), the regions of round white spots correspond to the double-chain structure, and regions with elongated white spots correspond to the triple-chain parts of the structure. Figures 1A and 1B show that the proportion of triple to double chains is highly variable from place to place. In Figure 1A the largest observed region that is composed of triple chains is 23 chain widths or about 311 Å. In Figure 1B the largest double-chain region is 68 chain widths or about 612 Å. The diffraction pattern (Fig. 1C) from the area with high triple-chain concentration, which includes the area shown in Figure 1A, clearly shows diffraction maxima for the triple-chain structure (small arrows). The diffuseness of the diffraction maxima is due to the extremely narrow width of lamellae in the disordered double- and triple-chain interlayerings. Since the

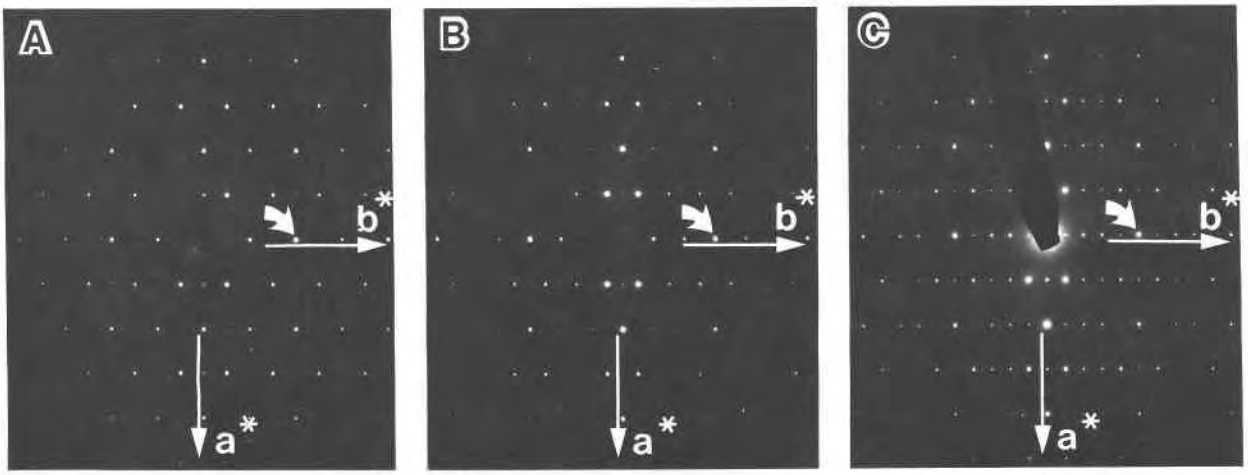

Fig. 2. Selected-area electron-diffraction photographs of anthophyllite (A), jimthompsonite (B), and chesterite (C) in [001] orientation. The heavy arrows denote, respectively, the (040), (060) and (0,10,0) diffraction maxima.

(040) diffraction maxima of anthophyllite and the (060) diffraction maxima of jimthompsonite (heavy arrow) are superimposed and represent the 4.5-Å subperiod for all the multiple chains, these and corresponding diffraction maxima are sharper. In addition to the disordered or mixed intergrowth of double- and triple-chain units, areas of undisturbed double-chain units (anthophyllite), alternating double- and triple-chain units (chesterite), and triple-chains units (jimthompsonite) on the order of several thousand ångströms in width were observed. The electron-diffraction patterns for anthophyllite, chesterite, and jimthompsonite are shown in Figure 2. Multiple chains with multiplicity greater than three (i.e., quadruple chains or wider) were only rarely observed. Intrastructural termination of the multiple chains, which were described as zippers by Veblen and Buseck (1979), are also extremely rare in this sample.

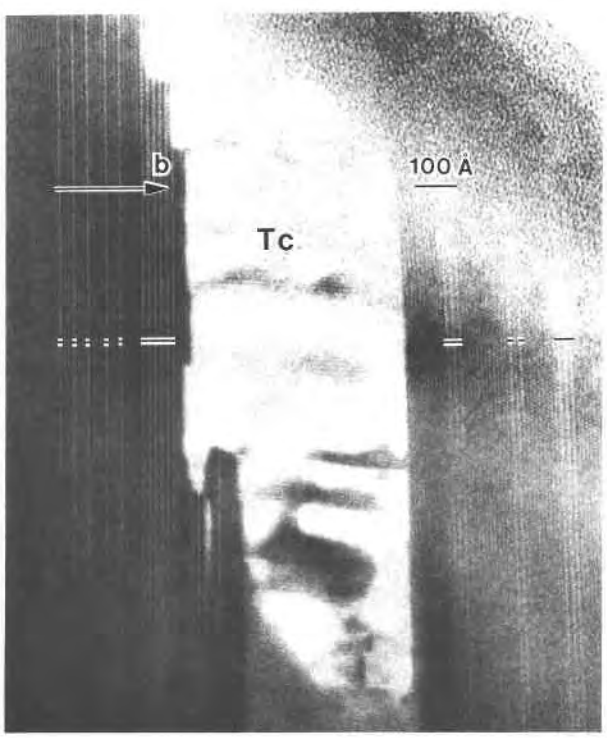

Fig. 3. Bright-field image of biopyriboles in [001] projections that show talc (Tc) replacement of triple- and double-chain pyribole. Bars in parts A and B denote triple-chain regions, and unmarked areas are double-chain regions.

A sheet silicate, which was not seen with the optical microscope, was found as a lamella within the pyribole grains (Fig. 3). Qualitative energy-dispersive analyses done in the HRTEM indicate that it is composed mostly of Si, Mg, and Fe and lacks Na and K. On the basis of its approximately 9.1-Å spacing between the sheets and the compositional data, this sheet silicate is assumed to be talc and seems to be replacing concurrently the double and triple chains (Fig. 3).

Mineral chemistry

Electron-microprobe analyses were necessarily done before the HRTEM work confirmed the presence of triple-chain lamellae, since ion-thinned samples are not suitable for further electron-microprobe analyses. At the time the qualitative analyses were made, the presence of triple-chain lamellae in the "anthophyllite" was suspected from the optical properties described above. Analyses were made at points on the crystal that spanned the entire range of observed interference colors. The lower-order interference colors should represent double-chain rich areas and the higher-order ones triple-chain rich areas; in fact, the chemical variations, which are discussed below and ascribed to varying proportions of double- and triple-chain parts of the crystal, correlated excellently with the variations in interference color, and the subsequent HRTEM observations.

TABLE 2. Representative analyses of anthophyllite (ANTH), disordered pyribole (MIXED), and jimthompsonite (JT)

	ANTH		MIXED				JT	
SiO_2	57.51		57.53	57.86	58.16		58.24	
TiO_2	0.00		0.03	0.04	0.02		0.04	
Al_2O_3	1.04		1.10	1.13	1.23		1.34	
Cr_2O_3	0.01		0.00	0.02	0.00		0.00	
FeO	11.75		11.49	10.84	10.09		9.15	
MnO	0.21		0.25	0.20	0.20		0.16	
MgO	26.52		26.54	26.56	26.67		27.04	
NiO	0.00		0.00	0.00	0.00		0.00	
ZnO	0.52		0.30	0.26	0.35		0.25	
CaO	0.52		0.45	0.42	0.38		0.35	
Na_2O	0.13		0.19	0.16	0.19		0.29	
K_2O	0.01		0.01	0.00	0.00		0.00	
Total	98.22		97.89	97.49	97.29		96.86	
	Cations per 23 oxygens						Cations per 34 oxygens	
Si	7.898	Si	7.898	7.908	7.948	7.975	7.981	Si 11.797
Al	0.102							Al 0.203
Sum	8.000							Sum 12.000
		Al	0.168	0.178	0.183	0.199	0.216	
Al	0.066							Al 0.117
Ti	0.000	Ti	0.000	0.003	0.004	0.002	0.004	Ti 0.006
Cr	0.001	Cr	0.001	0.000	0.002	0.000	0.000	Cr 0.000
Mg	5.429	Mg	5.429	5.438	5.439	5.452	5.524	Mg 8.165
Fe^{2+}	1.349	Fe^{2+}	1.349	1.321	1.245	1.157	1.049	Fe^{2+} 1.550
Mn	0.024	Mn	0.024	0.029	0.023	0.023	0.019	Mn 0.027
Zn	0.053	Zn	0.053	0.030	0.026	0.035	0.025	Zn 0.037
Ca	0.077	Ca	0.077	0.066	0.062	0.056	0.051	Ca 0.076
Na	0.001							Na 0.022
Sum	7.000							Sum 10.000
Na	0.034	Na	0.035	0.051	0.043	0.051	0.077	Na 0.092
K	0.002	K	0.002	0.000	0.000	0.000	0.000	K 0.000
Sum	0.036							Sum 0.092
Total	15.036		15.036	15.026	14.976	14.949	14.946	22.094
X_{Mg}	0.801		0.801	0.805	0.814	0.825	0.840	0.840

Note: Oxides in weight percent. X_{Mg} = Mg/(Mg + Fe). ANTH and JT formulae are given twice, both with and without site distinctions.

Estimating analytical error (i.e., standard deviation of the mean) for either the anthophyllite-like or the jimthompsonite-like parts of these grains is difficult because of double- and triple-chain lamellar interlayering and was not done here. It is likely that even closely spaced analysis points contain variable proportions of double- and triple-chain units. Consequently, one cannot easily separate the effects of analytical error from compositional variation. In the diagrams discussed below, linear correlations were very good, and departures from a perfect linear fit probably reflect the analytical errors.

The most notable chemical variations are the systematic decrease in FeO,CaO, and the analytical total coupled with a complimentary increase in SiO_2, Al_2O_3, and MgO (Table 2, see also the cation values for these elements). These variations are almost certainly due to the variable double- to triple-chain ratios at different analytical points. Nevertheless, it is possible to ascertain which of these analyses most nearly represent anthophyllite and jimthompsonite.

To compare formulae, jimthompsonite is calculated on the basis of 23 instead of 34 oxygens. An ideal, Na-free jimthompsonite would have 14.882 cations per 23 oxygens and an equivalent anthophyllite would have 15.00 cations. As a result, analyses of mixed triple- and double-chain structures should have cation totals that lie between these two values (e.g., chesterite has an ideal 23-oxygen cation total of 14.930), and in principle, the 23-oxygen cation total could be used to estimate the relative proportions of double to triple chains present at the analysis point. However, the presence of Na or the effects of failure to account for Fe^{3+} will also cause the cation total to vary. The general sulfide-rich environment of the Orijärvi deposit suggests a reducing environment. In addition, the all-ferrous Fe formula of the coexisting spinel suggests that Fe^{3+} is absent. Consequently, Fe^{3+} was assumed to be absent.

Na could be assigned to either a glaucophane-like ($Na^{oct}Al^{oct}Mg^{oct}_{-1}Mg^{oct}_{-1}$) or an edenite-like ($Na^{A}Al^{tet}\square^{A}_{-1}Si^{tet}_{-1}$) substitution in both the double- and triple-chain parts of the structure. Na added by the glaucophane-like substitution will have no effect on the cation total (vertical arrows, Fig. 4), whereas each Na added by the edenite-like substitution will increase the cation total by a number equal to the Na (and K) at the A site (i.e., 15 + Na cations at A for anthophyllite and 14.883 + Na cations

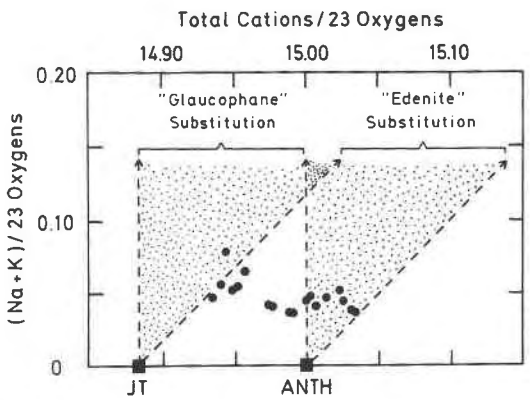

Fig. 4. Plot of Na + K versus total cations based on 23-oxygen formulae for the analyzed pyriboles (filled circles). Filled squares represent ideal 23-oxygen cation totals (anhydrous) for anthophyllite (ANTH) and jimthompsonite (JT), 15.000 and 14.882 respectively. Vertical and inclined arrows show possible (Na + K) vs. total cation variations due to variable amounts of glaucophane-like ($Na^{oct}Al^{oct}Mg^{oct}_{-1}\ Mg^{oct}_{-1}$) or edenite-like ($Na^{A}Al^{tet}\square^{A}_{-1}Si^{tet}_{-1}$) substitution in jimthompsonite or anthophyllite. Stippled areas represent (Na + K) vs. total cation values for various ratios of glaucophane- to edenite-like substitutions in anthophyllite and jimthompsonite.

at A for jimthompsonite; shown as inclined arrows, Fig. 4). As a result, the correct cation total either for Na-bearing anthophyllite or for Na-bearing jimthompsonite will lie somewhere between the glaucophane-like and edenite-like substitution trends (stippled areas, Fig. 4) at the specific number of Na cations in an individual analysis. The range of the possible cation totals increases as the amount of Na in the analyzed grain increases, and the correct cation value could only be determined if the ratio of the glaucophane to edenite substitution is known.

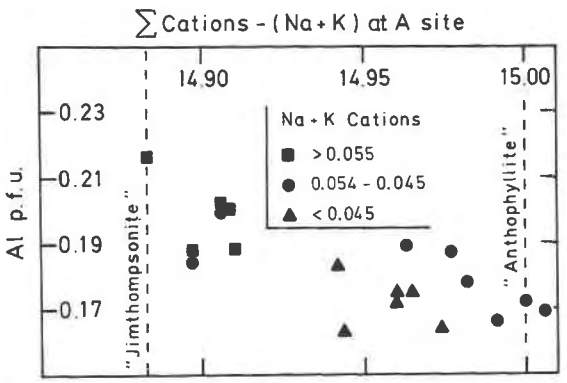

Fig. 5. Plot of Al per formula unit (pfu) vs. total cations minus (Na + K) in the A site [Σ cations − (Na + K)] based on 23-oxygen formulae for the analyzed pyriboles. Filled triangles, circles, and squares indicate different ranges of Na content in the analyses. The dashed vertical lines indicate the ideal 23-oxygen totals of jimthompsonite (14.882) and anthophyllite (15.000) assuming that 80.7% of the Na cations are incorporated via the edenite-like substitution ($NaAl^{tet}\square^{A}_{-1}Si^{tet}_{-1}$).

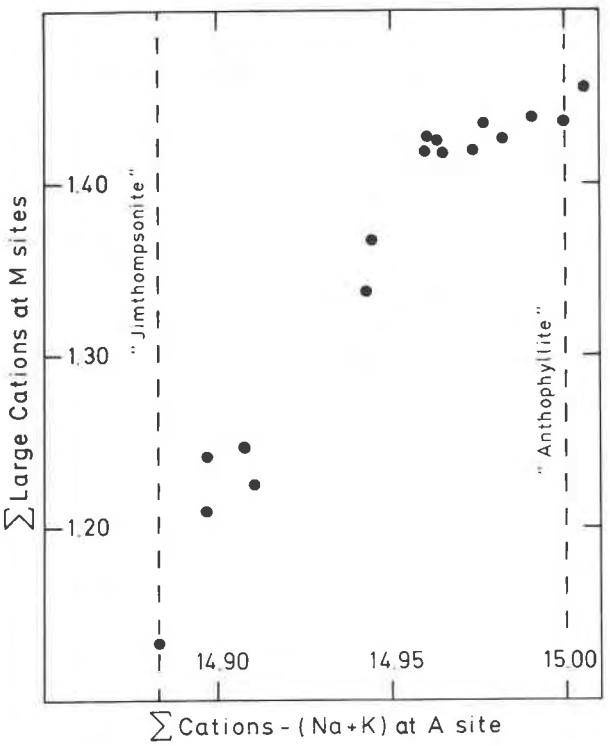

Fig. 6. Plot of total large cations [Σ (Ca + Mn + Fe^{2+})] vs. total cations minus (Na + K) in the A site [Σ cations − (Na + K)] based on 23-oxygen formulae for the analyzed pyriboles. Filled circles represent individual analyses. The dashed vertical lines indicate the ideal 23-oxygen totals of jimthompsonite (14.882) and anthophyllite (15.000) assuming that 80.7% of the Na cations are incorporated via the edenite-like substitution ($Na^{A}Al^{tet} = \square^{A}_{-1}Si^{tet}_{-1}$).

Site-occupancy determinations for orthoamphiboles (Papike and Ross, 1970) show that most of the Na is at the A site; this is probably true for the triple-chain silicates and is supported by difference Fourier maps that show electron densities at the A site (Veblen and Burnham, 1978b). Consequently, one might speculate that both the Na-bearing double- and triple-chain parts would give analyses that lie close to the edenite-like substitution trend.

The analyses from the pyribole grain in this study are bounded by the ideal edenite trends for anthophyllite and jimthompsonite (Fig. 4). At the anthophyllite end of the data-point cluster in Figure 4, the analysis points closely approach the edenite trend, which represents a crystallochemical limit and suggests that the Na in some of the anthophyllite resides almost exclusively at the A site. At the other end of the data-point cluster, several analyses approach the edenite trend for jimthompsonite, and one analysis enters the stippled area. This also suggests that most of the Na is at the A site of the triple-chain silicate, because analyses of areas rich in triple-chains that contain significant octahedral Na should overlap farther into the stippled area in Figure 4. Formulae with the highest and lowest cation totals are thought to represent analyses of

Na-bearing anthophyllite and Na-bearing jimthompsonite, respectively, and analyses with intermediate cation values would represent disordered areas with varying proportions of double and triple chains (Table 2). The analysis that was chosen as representative of jimthompsonite contains the highest Na and Al of all the pyribole analyses; it is the only analysis to fall within the jimthompsonite (stippled area) in Figure 4, which means part of the Na is assigned to the octahedral sites (Table 2). The analysis with the highest cation total per 23 oxygens was chosen as the most likely anthophyllite analysis.

In order to illustrate chemical differences between the two types of structures, a common basis for comparison must be used as a measure of the relative proportions of double to triple chains. Several choices for this basis exist, and they include (1) total cations; (2) total cations exclusive of Na + K; and (3) total cations exclusive of A-site cations, which could be determined from the Na^A/Na^M ratio that is taken from either the anthophyllite or the jimthompsonite formulas. Comparisons in Figures 5 and 6 use total cations exclusive of A-site cations. The Na assigned to the A site is 80.7% of the total Na atoms pfu and is based on the $Na^A/(Na^A + Na^M)$ of the jimthompsonite analysis.

The Al contents of the pyriboles are low (0.220 per 23 oxygens), but Figure 5 shows a slight relative Al enrichment in areas with abundant triple chains. The analysis points (Fig. 5) are divided into three broad categories based on Na content. The increase in Al seems to correlate roughly with higher Na. This correlation is probably due to the edenite-like substitution and suggests that Na and Al are more easily incorporated into the triple-chain structure than into the double-chain structure. This may be due to the fact that the proportion of A sites and tetrahedral sites relative to octahedral sites (see Veblen, 1981, Fig. 8) is larger in jimthompsonite than in anthophyllite.

Cation ordering between the distorted and regular octahedral sites of the pyriboles has been discussed in detail by Veblen (1981), and a plot of the sum of the large cations vs. the modified cation total for these samples also shows the preferential ordering of the large cations into the distorted and nearly equivalent octahedra M4 (amphibole) and M5 (jimthompsonite) (see Veblen and Burnham, 1978b). Figure 6 shows a linear decrease in large cations from about 1.440 (anthophyllite) to 1.100 (jimthompsonite), which can be explained by the differences in the ratios of distorted (M4 or M5) to regular M polyhedra in the two structures. In amphiboles, the ratio of M4 to smaller M sites is 2:5, and in jimthompsonite, the ratio of M5 to other M sites is 2:8. Consequently, the double-chain areas of the grain contain more total Ca + Mn + Fe^{2+}. Assuming that the Fe-Mg distribution between the distorted M polyhedra (dM) and the regular M polyhedra (rM) are similar in anthophyllite and jimthompsonite at the temperature of jimthompsonite formation, the intersite distribution coefficient $[(K_d)^{dM\text{-}rM}_{Fe\text{-}Mg}]$ would have been the same in both parts. Providing that no redistribution of Fe and Mg occurred among the phases, the differences in the numbers of dM and rM polyhedra and total Fe^{2+} contents can be used to derive the $(K_d)^{dM\text{-}rM}_{Fe\text{-}Mg}$ at the conditions of jimthompsonite formation. After assigning Ca, Mn, and Na^M to the distorted polyhedra and Al^{VI}, Cr, Ti, and Zn to the regular polyhedra (partially blocking these polyhedra to Fe^{2+} and Mg), anthophyllite gives

$$1.898Fe^{2+}_{dM} + 4.911Fe^{2+}_{rM} = 1.349Fe^{2+}_{total}$$

and jimthompsonite gives

$$1.875Fe^{2+}_{dM} + 7.841Fe^{2+}_{rM} = 1.550Fe^{2+}_{total}.$$

Solving these two equations simultaneously gives the Fe content (X_{Fe}) of the distorted polyhedra (0.522) and the regular polyhedra (0.073), which can be used to obtain the $(K_d)^{dM\text{-}rM}_{Fe\text{-}Mg}$ as follows:

$$\begin{aligned}(K_d)^{dM\text{-}rM}_{Fe\text{-}Mg} &= (X^{dM}_{Fe}X^{rM}_{Mg})/(X^{dM}_{Mg}X^{rM}_{Fe}) \\ &= (0.522 \cdot 0.927)/(0.478 \cdot 0.073) \\ &= 13.868,\end{aligned}$$

and $\ln[(K_d)^{dM\text{-}rM}_{Fe\text{-}Mg}] = 2.630$.

Work by Seifert (1977) on anthophyllite has shown that the $\ln[(K_d)^{dM\text{-}rM}_{Fe\text{-}Mg}]$ is extremely temperature dependent. On the basis of the temperature vs. $\ln[(K_d)^{dM\text{-}rM}_{Fe\text{-}Mg}]$ correlations from Seifert's work, the $\ln[(K_d)^{dM\text{-}rM}_{Fe\text{-}Mg}]$ value obtained from the anthophyllite-jimthompsonite data suggests a metamorphic temperature near 600°C, in general agreement with the 550–630°C temperature of metamorphism suggested by Schreurs (1985). It should be noted that given the strong temperature dependence of $(K_d)^{dM\text{-}rM}_{Fe\text{-}Mg}$, intersite redistribution within both the anthophyllite and jimthompsonite probably has occurred. However, this will have no effect on the above calculation, which should reflect the $(K_d)^{dM\text{-}rM}_{Fe\text{-}Mg}$ value at the last temperature of equilibrium between the double- and triple-chain parts of the structure.

Concluding remarks

The TEM images have shown that the pyribole studied here consists almost completely of double and triple chains, which are present in variable proportions in the different parts of the grain. With this knowledge, chemical variations in analyses of a single pyribole grain can be attributed to different proportions of double to triple chains at the analysis point. This work shows regular and significant chemical changes between double- and triple-chain-rich areas and is in agreement with the kinds of chemical variations observed by Veblen and Burnham (1978a) and Veblen (1981).

Acknowledgments

This work was supported by Grant Se 302/18-2 from the Deutsche Forschungsgemeinschaft (the German Research Foundation), and their support is gratefully acknowledged. We thank F. Seifert, D. R. Veblen, J. B. Thompson, and F. C. Hawthorne, whose comments and suggestions greatly improved this manuscript. D. Ackermand and T. Lund aided with microprobe analyses. B. Mader, B. Mackewic, and B. Burmeister provided invaluable assistance in preparation of line drawings and photographs.

References

Akai, J. (1982) Polymerization process of biopyriboles in metasomatism at the Akatani ore deposit, Japan. Contributions to Mineralogy and Petrology, 80, 117–131.

Berge, J.W. (1978) A re-examination of the association of magnesium and massive sulphide ores. Geologiska Föreningens i Stockholm Förhandlingar, 100, 155–170.

Buseck, P.R., and Iijima, S. (1974) High resolution electron microscopy of silicates. American Mineralogist, 59, 1–21.

Cressey, B.A., Whittaker, E.J.W., and Hutchison, J.L. (1980) Electron microscopy of amphiboles along [001] (abs.). International Mineralogical Association, 12th General Meeting, Orléans, p. 94.

Eskola, P. (1914) On the petrology of the Orijärvi region in southwest Finland. Geological Survey of Finland Bulletin 40, 277 p.

Nakajima, Y., and Ribbe, P.H. (1980) Alteration of pyroxenes from Hokkaido, Japan, to amphibole, clays and other biopyriboles. Neues Jahrbuch für Mineralogie Monatshefte, 6, 258–268.

Nissen, H.-U., Wessicken, R., Woensdregt, C.F., and Pfeifer, H.R. (1979) Disordered intermediates between jimthompsonite and anthophyllite from the Swiss Alps. In T. Mulvey, Ed. Electron microscopy and analysis, 1979 (EMAG '79). Institute of Physics (Bristol) Conference Series 52, 99–100.

Papike, J.J., and Ross, M. (1970) Gedrites: Crystal structures and intracrystalline cation distributions. American Mineralogist, 55, 1945–1972.

Robinson, Peter, Spear, F.S., Schumacher, J.C., Laird, J., Klein, C., Evans, B.W., and Doolan, B.L. (1982) Phase relations of metamorphic amphiboles: Natural occurrence and theory. Mineralogical Society of America Reviews in Mineralogy, 9B, 1–227.

Schreurs, J. (1985) Prograde metamorphism of metapelites, garnet-biotite thermometry and prograde changes of biotite chemistry in high-grade rocks of West Uusimaa, southwest Finland. Lithos, 18, 69–80.

Schumacher, J.C. (1983) Stratigraphic, geochemical, and petrologic studies of the Ammonoosuc Volcanics, north-central Massachusetts and southwestern New Hampshire. Ph.D. thesis, University of Massachusetts, Amherst, 237 p.

Seifert, F. (1977) Equilibrium Mg-Fe^{2+} cation distribution in anthophyllite. American Journal of Science, 278, 1323–1333.

Simonen, A. (1980) The Precambrian of Finland. Geological Survey of Finland Bulletin 304, 58 p.

Spear, F.S., Hazen, R.M., Rumble, D., III. (1981) Wonesite: A new rock-forming silicate from the Post Pond Volcanics, Vermont. American Mineralogist, 66, 100–105.

Veblen, D.R. (1981) Non-classical pyriboles and polysomatic reactions in biopyriboles. Mineralogical Society of America Reviews in Mineralogy, 9A, 189–236.

Veblen, D.R., and Burnham, C.W. (1975) Triple-chain biopyriboles: Newly discovered intermediate products of the retrograde anthophyllite-talc transformation, Chester, VT (abs.). EOS, 56, 1076.

——— (1976) Biopyriboles from Chester, Vermont: The first mixed-chain silicates. Geological Society of America Abstracts with Programs, 8, 1153.

——— (1978a) New biopyriboles from Chester, Vermont: I. Descriptive mineralogy. American Mineralogist, 63, 1000–1009.

——— (1978b) New biopyriboles from Chester, Vermont: II. The crystal chemistry of jimthompsonite, clinojimthompsonite, and chesterite, and the amphibole-mica reaction. American Mineralogist, 63, 1053–1073.

Veblen, D.R., and Buseck, P.R. (1979) Chain-width order and disorder in biopyriboles. American Mineralogist, 64, 687–700.

——— (1981) Hydrous pyriboles and sheet silicates in pyroxenes and uralites: Intergrowth microstructures and reaction mechanisms. American Mineralogist, 66, 1107–1134.

Veblen, D.R., Buseck, P.R., and Burnham, C.W. (1977) Asbestiform chain silicates: New minerals and structural groups. Science, 198, 359–365.

Whittaker, E.J.W., Cressey, B.A., and Hutchison, J.L. (1981a) Terminations of multiple-chain lamellae in grunerite asbestos. Mineralogical Magazine, 44, 27–35.

——— (1981b) Edge dislocations in fibrous grunerite. Mineralogical Magazine, 44, 287–291.

Yau, Yu-Chi, and Peacor, D.R. (1985) Wide-chain Ca-pyribole and actinolite intergrowths in primary euhedral crystals from the Salton Sea geothermal field, California (abs.). EOS, 66, 373.

Manuscript received November 1, 1985
Manuscript accepted November 7, 1986